

Old Carbon, New Insights: Thermal Reactivity and Bioavailability of Saltmarsh Soils

Alex Houston¹, Mark H Garnett², and William E N Austin^{1,3}

1. Department of Geography and Sustainable Development, University of St Andrews, St Andrews, KY16 9AL, United Kingdom
2. NEIF Radiocarbon Laboratory, Scottish Universities Environmental Research Centre, East Kilbride, G75 0QF, United Kingdom
3. Scottish Association of Marine Science, Oban, PA37 1QA, United Kingdom

Correspondence to: Alex Houston (ah383@st-andrews.ac.uk)

Abstract

Saltmarshes are globally important coastal wetlands which can help to mitigate the impacts of climate change. They accumulate organic carbon from both modern and aged sources through in-situ biological production and the capture of ex-situ sources which are deposited during tidal inundation. Previous studies have found that long-term organic carbon storage in saltmarsh soils is driven by the net contribution from the older fraction, implying that the inputs of young organic carbon derived from in situ production are recycled at a faster rate.

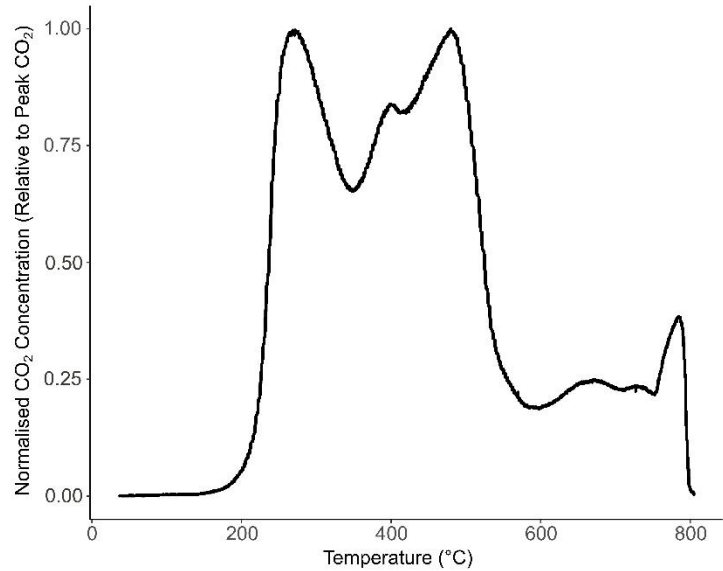
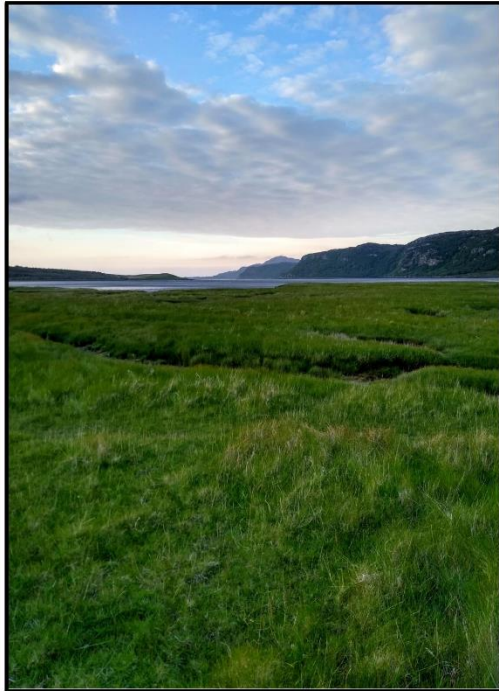
Using ramped oxidation, we assessed the composition (¹⁴C and ¹³C) of saltmarsh soil carbon pools defined by their thermal reactivity. By relating ¹⁴C measurements of the soil carbon pools to CO₂ respired in aerobic incubations of the same soils, we provide the first empirical evidence linking the thermal reactivity of saltmarsh soil organic carbon with its bioavailability for remineralization.

We found that old (¹⁴C-depleted) carbon dominates the thermally recalcitrant organic carbon pools, whereas the thermally labile carbon is composed of younger organic carbon sources. In most cases, the ¹⁴C content of the most thermally labile carbon pool was closest to the previously reported ¹⁴C content of the CO₂ evolved from aerobic incubations of the same soils, implying that the bioavailability of saltmarsh soil organic carbon to remineralisation in oxic conditions is closely related to its thermal lability.

Our results highlight the importance of saltmarshes as stores of both old, thermally recalcitrant organic carbon, as well as younger, thermally labile organic carbon that is vulnerable to decomposition under oxic conditions. Management interventions (e.g. rewetting by tidal inundation)

to limit the exposure of saltmarsh soils to elevated oxygen availability may help to protect and conserve these stores of thermally labile organic carbon and hence limit CO₂ emissions. We also present evidence to support the inclusion of thermally labile allochthonous OC stored in saltmarsh soils in additionality assessments for projects which aim to prevent the drainage of saltmarshes, with relevance to international carbon crediting projects and National GHG Inventories.

Graphical Abstract



1 **1. Introduction**

2 Saltmarshes accumulate organic carbon (OC) of variable age and reactivity into their soils. A
3 portion of this OC is stored for millennia, providing a climate regulation service, and some is
4 returned to the atmosphere or laterally exported (Komada et al., 2022; Macreadie et al., 2021).
5 Saltmarshes also accumulate and produce inorganic carbon (IC) but the climate regulation
6 service of this is currently under debate and unclear (Granse et al., 2024; Van Dam et al., 2021).

7 To understand the role of saltmarsh soils in carbon cycling and their potential for climate
8 mitigation through targeted management interventions, much research has focussed on
9 determining the autochthonous (in-situ) and allochthonous (ex-situ, trapped during tidal
10 inundation from terrestrial and marine sources) contributions to saltmarsh soils, with the
11 accumulation of autochthonous OC as a direct sequestration of carbon from the atmosphere,
12 reducing the amount of atmospheric greenhouse gases (GHGs) (Macreadie et al., 2019; Saintilan
13 et al., 2013; Van de Broek et al., 2018). The accumulation of allochthonous OC, originally
14 sequestered outside the saltmarsh area, does not directly reduce atmospheric GHGs, but can
15 represent a source of avoided emissions if it remains stored in the saltmarsh soil for longer than
16 in an alternative depositional environment (Howard et al., 2023). Evidence to determine whether
17 this is the case or not, and under what scenarios, has proven challenging to obtain (Geraldini et al.,
18 2019; Houston et al., 2024a). OC pools with distinct biological turnover times may instead
19 provide greater insights into the soil carbon residence time and therefore the climate mitigation
20 achieved through targeted management interventions to retain that carbon (Sanderman and
21 Grandy, 2020).

22 Ramped oxidation (RO) and ramped pyrolysis oxidation (RPO) have been used to estimate the
23 thermal reactivity and biological turnover time of soil and sediment OC (Hemingway et al., 2017b;
24 Plante et al., 2011; Rosenheim et al., 2008). RO and RPO involve measuring the quantity of CO₂
25 evolved as a sample is increasingly heated at a constant rate in an atmosphere containing oxygen
26 (e.g., Hemingway et al., 2017b; Plante et al., 2011; Stoner et al., 2023), or other gases, typically
27 Helium (e.g., Rosenheim et al., 2008). The temperature at which CO₂ is thermally-evolved is
28 related to the activation energy required to thermally decompose C (Hemingway et al., 2017b),
29 which is also an estimate of the energy required for biological degradation of OC (Peltre et al.,
30 2013; Plante et al., 2013). CO₂ evolved at low temperatures is derived from soil OC pools with a
31 greater thermal lability than CO₂ evolved at higher temperatures (Peltre et al., 2013; Rosenheim
32 et al., 2008). OC thermal reactivity pools can be examined by collecting the evolved CO₂ from set
33 temperature ranges with distinct thermal reactivities and measuring the ¹⁴C (age) and ¹³C content

34 (Rosenheim et al., 2008), which can then be related to the activation energy required to thermally
35 decompose those C sources (Hemingway et al., 2017b).

36 The ^{14}C content of the thermal reactivity pools provides insight into the turnover time of each pool,
37 with past research showing that the oldest soil organic matter (OM) (most depleted ^{14}C content)
38 tends to dominate the most thermally recalcitrant fractions (Bao et al., 2019b; Plante et al., 2013;
39 Stoner et al., 2023). Similar results have been found for saltmarsh soils (Luk et al., 2021). Young
40 OC, which can be autochthonous or allochthonous (Van de Broek et al., 2018), has been found
41 to turnover at a faster rate than old OC in saltmarsh soils (Komada et al., 2022; Van de Broek et
42 al., 2018), implying that young OC may tend to be more thermally labile than old OC for saltmarsh
43 soils.

44 The ^{13}C content of the thermal reactivity pools can also provide insight as to whether the source
45 of OC has an influence on turnover time. Previous work has found that the ^{13}C content of evolved
46 CO_2 tends to be more enriched at higher temperatures due to greater contributions from ^{13}C -
47 enriched, degraded/microbially derived OC (Luk et al., 2021; Sanderman and Grandy, 2020;
48 Stoner et al., 2023). Similarly, comparisons of the isotopic composition of thermally-defined OC
49 pools to their chemical properties have found that thermally labile OC is derived from mostly
50 lipids and polysaccharides, whereas OC with a higher thermal recalcitrance is derived from a
51 greater proportion of phenolic and aromatic compounds (Sanderman and Grandy, 2020). The
52 thermal reactivity of soil and sediment OC is also influenced by the formation of organo-mineral
53 complexes, which can physically and chemically stabilise OC (Bianchi et al., 2024; Hemingway
54 et al., 2019). Mineral-associations can increase the energy required for decomposition and have
55 been found to increase thermal recalcitrance and to slow turnover times of soil and sediment OC
56 (Hemingway et al., 2019; Stoner et al., 2023).

57 Crucially, the biological availability (bioavailability) of OC for decomposition, and hence its
58 biological turnover time, is related to the prevailing environmental conditions as well as thermal
59 reactivity (Hemingway et al., 2017b; Schmidt et al., 2011). For example, increased hydrodynamic
60 energy can destabilise organo-mineral complexes and increase the bioavailability of previously
61 stable OC (Spivak et al., 2019). Similarly, increased oxygen availability can decrease the energy
62 requirement for microbes to decompose molecularly recalcitrant OC, causing it to be
63 remineralised at a faster rate (Noyce et al., 2023).

64 Houston et al. (2024b) found that young OC stored in saltmarsh soils was preferentially respired
65 as carbon dioxide (CO_2) during aerobic incubation experiments, but that a portion of the respired
66 CO_2 was produced from an aged (^{14}C -depleted), allochthonous source. It is possible that this

67 CO₂ could have been respired from thermally labile as well as thermally recalcitrant soil OC
68 sources because the increased oxygen availability of the incubations potentially facilitated the
69 degradation of OC which was previously stable in the low-oxygen environment of typical
70 saltmarsh soils (Noyce et al., 2023).

71 The isotopic composition of RO thermal reactivity fractions can be compared to the isotopic
72 composition of the CO₂ that is evolved biologically during incubations of equivalent samples to
73 determine whether or not the age of the most biologically- and thermally-reactive OC pools
74 match. Here, we present the first measurements of the ¹³C and ¹⁴C content of CO₂ derived from
75 saltmarsh soils using RO, and the first comparison of these to the ¹⁴C content of biologically
76 evolved CO₂ from the same soils (Houston et al., 2024b). We hypothesised that the thermally
77 labile C pools would be composed of younger C than the thermally recalcitrant pools, and that
78 the CO₂ evolved from saltmarsh soils exposed to oxic conditions (Houston et al., 2024b) are from
79 a predominantly thermally labile OC pool.

80 **2. Methods**

81 **2.1. Field site and sample collection**

82 Three saltmarsh soil cores (T1-3) were retrieved ca. 30 m apart from the lower marsh zone from
83 Skinflats (SK), an estuarine saltmarsh in Scotland (56° 3'34.04"N, 3°43'59.16"W), as detailed in
84 Houston et al. (2024b). Field methods and laboratory sub-sampling procedures are described in
85 detail in Houston et al. (2024b). Briefly, the cores were split into 1 cm thick slices as follows: core
86 T1 (0-1 cm, 5-6 cm, and 18-19 cm); T2 (0-1 cm, 5-6 cm, and 15-16 cm), and T3 (0-1 cm, 5-6 cm,
87 and 19-20 cm) (with the deepest sample from each core being the deepest retrieved sample from
88 the 20 cm length of the corer. On the occasions when a full core was not retrieved, the deepest
89 retrieved soil was used). Each slice was subsequently divided to provide sample material for the
90 RO procedure, and for aerobic laboratory incubations from which the biologically evolved CO₂
91 was collected for ¹³C and ¹⁴C analysis (Houston et al., 2024b).

92 **2.2. Ramped oxidation**

93 The RO sub-samples were individually dried to constant mass before milling to a fine powder to
94 homogenise and limit potential shielding effects from aggregates. Unlike most RO and RPO
95 studies (e.g., Hemingway et al., 2017b), we did not remove carbonates from our samples. Acid
96 treatment, which is required to remove carbonates from samples has been demonstrated to
97 result in losses from the thermally labile OC fraction (Bao et al., 2019a), and affect the isotopic
98 values of the lower temperature fractions (Rosengard et al., 2025). A loss of labile OC for our
99 samples could seriously impact the interpretations in our study, and our ability to compare

100 the ^{14}C content of the CO_2 respired from bulk (untreated) soils in the incubation experiments
101 (Houston et al., 2024b) to the ^{14}C content of the RO thermal fractions.

102 The samples were sent to the NEIF Radiocarbon Laboratory for RO, which is described in Garnett
103 et al. (2023). The RO procedure involved two stages, a first combustion to determine the
104 relationship between the rate of CO_2 evolution and temperature (thermogram), and a second
105 combustion where evolved sample gases were collected across defined temperature ranges, for
106 subsequent isotope analysis. For the first combustion, ca. 200 mg of dried and homogenized
107 sample material was weighed into a quartz vial which was inset into a quartz combustion tube,
108 which was subsequently placed into a furnace set initially to room temperature. The furnace was
109 progressively heated at a constant rate of 5°C per minute to 800°C in a stream of high purity
110 oxygen (N5.5, BOC, UK). Heating caused combustion of the sample and the evolution of gas
111 which was passed into a second quartz combustion tube containing platinised wool in a furnace
112 set to a constant temperature of 950°C . The platinised wool acted as a catalyst to ensure
113 complete combustion of the evolved gases. Upon exiting the secondary combustion chamber
114 the sample passed through a glass tube containing magnesium perchlorate desiccant to remove
115 moisture and subsequently the CO_2 concentration of the gas was measured using a non-
116 dispersive infrared CO_2 sensor (SprintIR[®]-WF-5, Gas Sensing Solutions, UK). The sample was
117 then passed out of the sensor unit and vented to the atmosphere.

118 The measured CO_2 concentration (normalised for sample mass) was plotted against temperature
119 to produce thermograms which were used to identify temperature ranges, which defined C
120 thermal reactivity pools for this study: $150\text{-}325^\circ\text{C}$, $325\text{-}425^\circ\text{C}$, $425\text{-}500^\circ\text{C}$, $500\text{-}650^\circ\text{C}$, and 650-
121 800°C .

122 For each sample, the required mass of material to evolve sufficient CO_2 ($> 3\text{ mL}$) for ^{14}C
123 measurement was calculated based on the thermogram. A new sub-set from the original dried
124 and homogenised sample was then re-run following the RO procedure outlined above, but
125 instead of venting to atmosphere, after its measurement the evolved CO_2 was collected into foil
126 gas bags based on the defined temperature ranges. CO_2 was collected for ^{13}C analysis from 650-
127 800°C , but sufficient CO_2 was evolved for ^{14}C analysis from this thermal fraction for only one
128 sample (T1 0.5 cm, Table A1) and we do not consider this fraction further because it is likely
129 dominated by carbonates and not relevant to the purpose of this study.

130 The foil gas bags (5 L Spout Pouch, <https://www.pouchshop.co.uk/>) used for sample collection
131 were sealed with one-hole rubber bungs into which a 0.6 cm diameter x 5 cm length stainless
132 steel tube was inserted. Isoversinic tubing (Saint Gobain, France) was fitted over the stainless

133 steel to connect it to a quick coupling (Colder Products Company, USA), which allowed
134 connection to the RO kit.

135 Prior to the RO CO₂ collection, all equipment was cleaned using a standardised procedure
136 (Garnett et al., 2023). All glassware was combusted at 900°C for a minimum of two hours, and all
137 couplings and connectors were washed in carbon-free detergent (Decon) and rinsed in Milli-Q
138 water. The foil gas bags were cleaned by repeatedly (3 times) filling with ca. 1 L high purity nitrogen
139 gas (Research Grade 99.9995% purity, BOC, UK) and evacuating with an air pump, over a period
140 of at least 24 hours (to aid out-gassing of CO₂). The final evacuation, immediately before
141 connecting to the RO rig, involved pumping out the bags with an SBA-5 CO₂ analyser (PPsystems,
142 USA) to ensure that the bags did not contain significant contamination. Before commencing a
143 sample combustion, the entire RO rig was checked for leaks and other potential sources of
144 contamination by measuring the CO₂ concentration in the oxygen carrier gas exiting the kit, using
145 the SBA-5 CO₂ analyser.

146 Within 3 days of combusting a sample, the evolved gas in each foil bag was connected to a
147 vacuum rig for cryogenic recovery of pure sample CO₂ by passing it through slush (-78°C; dry ice
148 and industrial methylated spirits) and then liquid nitrogen (-196°C) traps, under high vacuum (ca.
149 3×10^{-3} millibars). The sample CO₂ was then split into three aliquots: One for $\delta^{13}\text{C}$ analysis using
150 isotope ratio mass spectrometry (IRMS; Delta V, Thermo-Fisher, Germany), one for graphitisation
151 and subsequent AMS ¹⁴C analysis, and one for an archive back-up. The graphitised AMS samples
152 were measured for ¹⁴C content at the SUERC AMS Laboratory (see Ascough et al., 2024). The ¹³C
153 content ($\delta^{13}\text{C}$ -VPDB) was used to normalise the ¹⁴C results to a $\delta^{13}\text{C}$ of -25 ‰ to correct for
154 isotopic fractionation. Following convention, ¹⁴C results are presented as %Modern (fraction
155 modern x 100) and conventional radiocarbon ages (years BP, where 0 BP = AD 1950 and age = -
156 $8033 \times \ln (\% \text{Modern}/100)$).

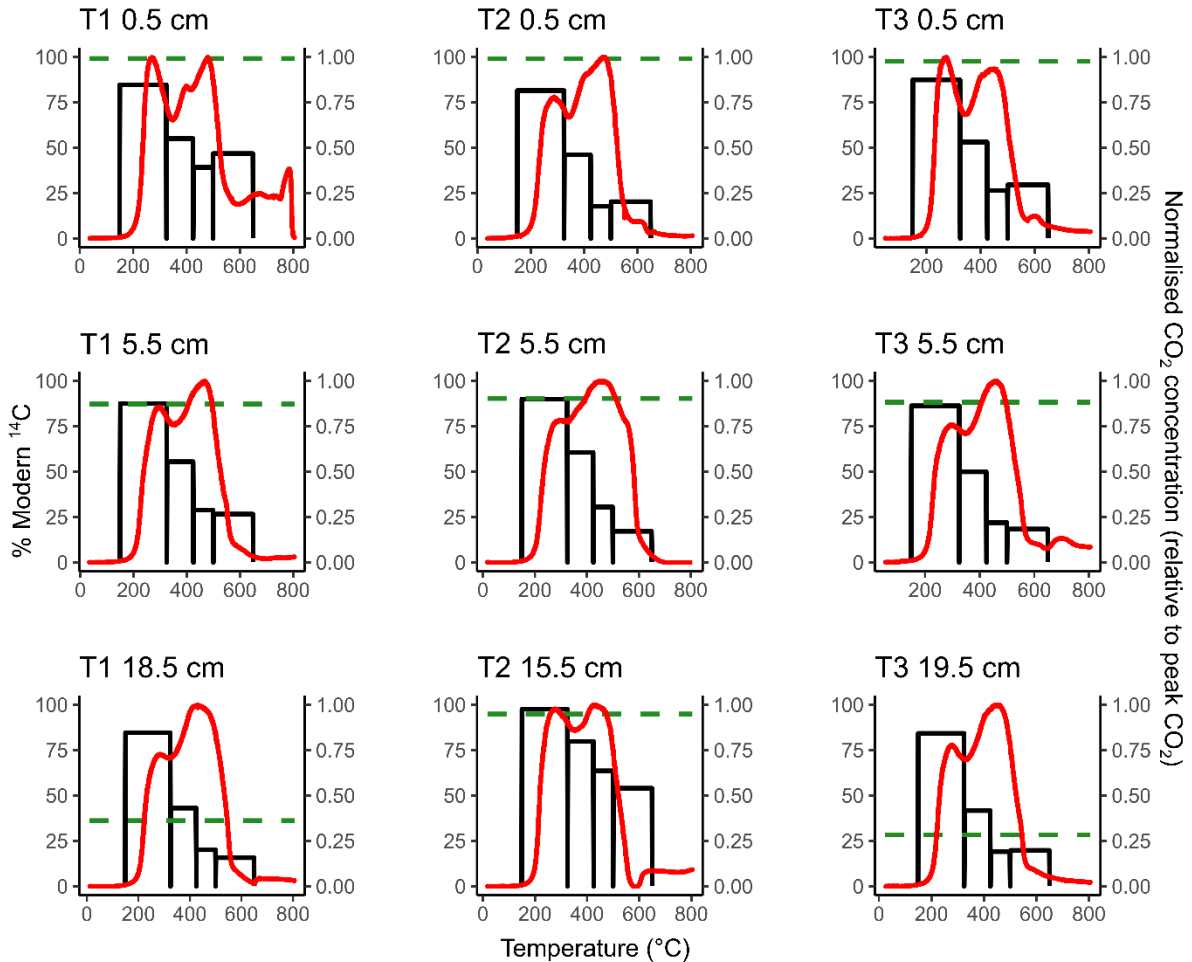
157 **2.3. Data Analysis**

158 Continuous activation energy distributions ($p(o,E)$) were modelled from thermograms using the
159 ‘*rampedpyrox*’ package in Python V3.8 (Hemingway, 2016; Hemingway et al., 2017b). The
160 distributed activation energy model calculates mean activation energies (μE) and the standard
161 deviation of activation energy (σE), which is a measure of the heterogeneity of bond strength, for
162 each temperature fraction which CO₂ was collected from. Mean μE , σE and activation energy
163 distribution ($p(o,E)$) are also calculated for each sample using the model. Further data analysis
164 and visualisation of thermograms and isotopic data was undertaken using RStudio V4.2.2 (R Core

165 Team, 2022). Statistical analyses (ANOVAs for parametric data; Kruskal-Wallis for non-
 166 parametric data) were undertaken in Sigmaplot V12.5.

167 **3. Results**

168 **3.1. Radiocarbon**



169

170 *Figure 1. Thermograms (red lines, right-hand y-axis) overlaying the ¹⁴C content of ramped*
 171 *oxidation fractions (black bars, left-hand y-axis) for each sample. The horizontal green dashed*
 172 *lines represent the ¹⁴C content of the CO₂ respired from the aerobic incubation experiments of*
 173 *Houston et al. (2024b).*

174 The ¹⁴C content of the RO fractions (Fig. 1, Table 1) were statistically similar between the 0.5 cm,
 175 5.5 cm, and deepest sample (T1 18.5 cm, T2 15.5 cm, T3 19.5 cm) depth increments for each of
 176 the temperature fractions (Kruskal-Wallis; p = 0.83, 0.38, 0.66, 0.99, for 150-325°C, 325- 425°C,
 177 425-500°C, 500-650°C, respectively). There were, however, clear differences in ¹⁴C contents
 178 between the temperature fractions, with ranges of 81.50-97.54 % Modern for 150-325 °C, 41.67-

179 79.80 % Modern for 325-425 °C, 17.67-63.56 % Modern for 425-500 °C, and 15.69-53.96 %
 180 Modern for 500-650 °C (Fig. 1, Table 1).

181 *Table 1. Radiocarbon concentration (% Modern) of RO temperature fractions and the CO₂*
 182 *produced in soil incubation experiments in Houston et al. (2024b). Errors are reported to one*
 183 *standard deviation from the mean. A sole ¹⁴C measurement for T1 0.5 cm 650-800 °C is reported*
 184 *in Table A1.*

	% Modern ¹⁴ C				Incubation CO ₂ (Houston et al., 2024b)
	150-325°C	325-425°C	425-500°C	500-650°C	
T1 0.5 cm	84.62 ± 0.44	55.02 ± 0.29	39.18 ± 0.21	46.75 ± 0.26	99.15 ± 0.45
T1 5.5 cm	87.51 ± 0.43	55.43 ± 0.28	28.76 ± 0.17	26.56 ± 0.16	87.18 ± 0.38
T1 18.5 cm	84.56 ± 0.44	43.06 ± 0.23	20.07 ± 0.13	15.70 ± 0.12	36.13 ± 0.36
T2 0.5 cm	81.50 ± 0.43	46.04 ± 0.24	17.67 ± 0.13	20.26 ± 0.14	98.97 ± 0.43
T2 5.5 cm	89.95 ± 0.42	60.55 ± 0.30	30.54 ± 0.17	17.11 ± 0.12	90.26 ± 0.40
T2 15.5 cm	97.53 ± 0.50	79.80 ± 0.41	63.56 ± 0.31	53.96 ± 0.27	94.86 ± 0.44
T3 0.5 cm	87.37 ± 0.45	53.09 ± 0.28	26.37 ± 0.15	29.55 ± 0.17	97.56 ± 0.43
T3 5.5 cm	86.23 ± 0.42	49.86 ± 0.25	21.87 ± 0.14	18.36 ± 0.12	88.22 ± 0.41
T3 19.5 cm	84.23 ± 0.41	41.67 ± 0.22	19.04 ± 0.13	19.76 ± 0.14	28.25 ± 0.37

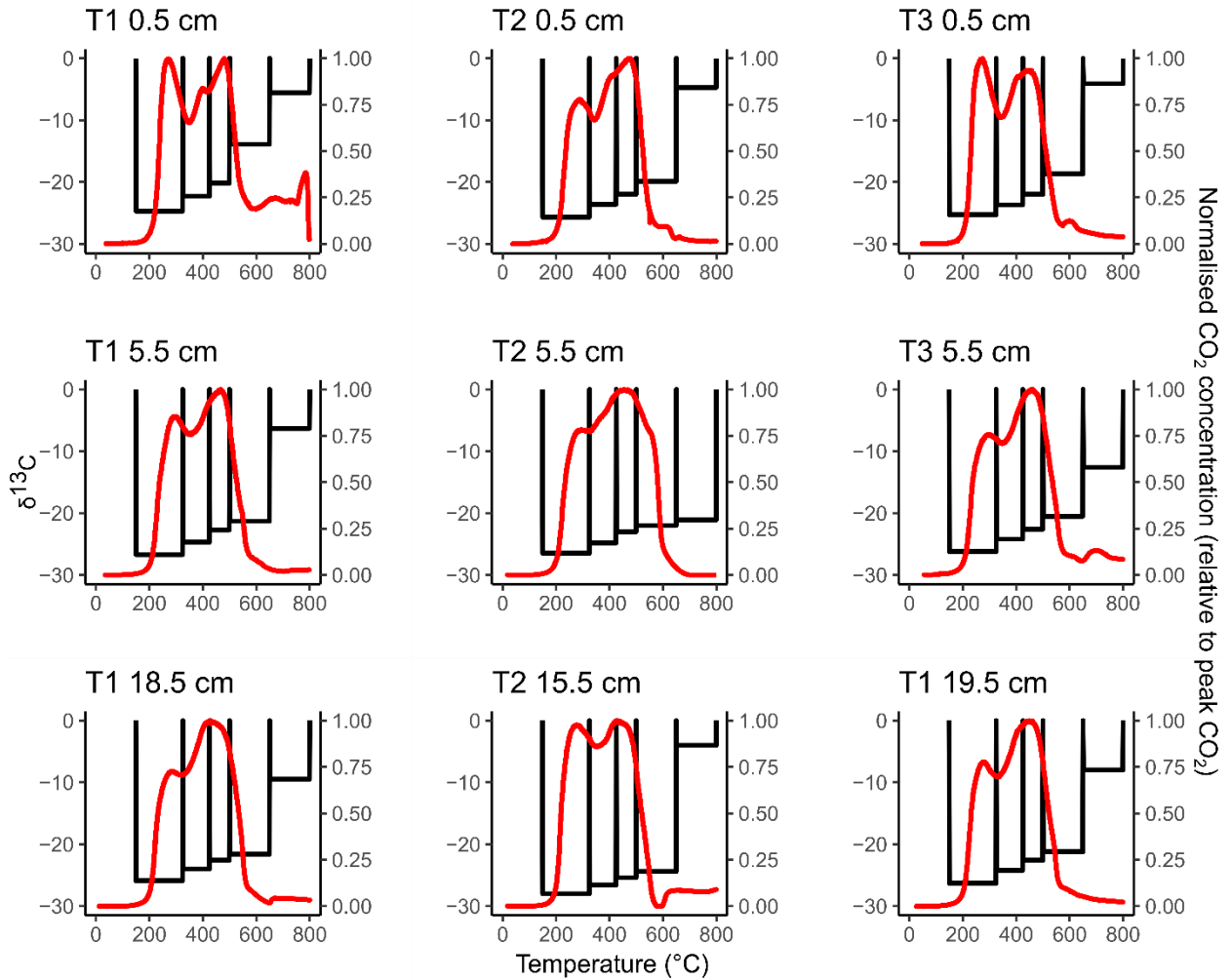
185

186 The RO samples were not pre-treated with acid, but the samples for bulk soil-¹⁴C were (Houston
 187 et al., 2024b), so we cannot verify that the weighted RO-¹⁴C contents amassed to the bulk soil ¹⁴C
 188 content. However, previous work using this analytical set-up have done this for other samples
 189 and shown that the combined RO fractions do equal the bulk isotope values (Garnett et al., 2023).

190 **3.2. δ¹³C**

191 There were no significant differences in the ¹³C content of the ramped oxidation fractions (Fig. 2,
 192 Table 2) between the depth increments (Kruskal-Wallis; p = 0.66, 0.63, 0.63, 0.44, 0.17, for 150-
 193 325 °C, 325-400 °C, 425-500 °C, 500-650 °C, 650-800 °C respectively). ¹³C contents followed the
 194 opposite trend to ¹⁴C contents with temperature, with ranges of -28.0 to -24.7 ‰ for 150-325 °C,

195 -26.6 to -22.3 ‰ for 325-425 °C, -25.4 to -20.2 ‰ for 425-500 °C, -24.4 to -13.9 ‰ for 500-650 °C,
 196 and -21.1 to -4.0 ‰ for 650-800 °C (Fig. 2, Table 2).



197

198 *Figure 2. Thermograms (red lines, right-hand y-axis) overlaying the ^{13}C content of the RO*
 199 *temperature fractions (black bars, left-hand y-axis) for each sample. Unlike Fig. 1, we did not*
 200 *attempt to relate the ^{13}C -RO to the ^{13}C content of the CO_2 respired in the incubation experiments,*
 201 *due to the potential for microbial fractionation during the incubation experiments.*

202

203 Table 2. $\delta^{13}\text{C}$ -VPDB‰ signature of the RO temperature fractions and the incubation
 204 experiments in Houston et al. (2024b). Errors are reported to one standard deviation from the
 205 mean.

	$\delta^{13}\text{C}$ - VPDB‰					Incubations (Houston et al., 2024b)
	150-325°C	325-425°C	425-500°C	500-650°C	650-800°C	
T1 0.5 cm	-24.7 ± 0.1	-22.3 ± 0.1	-20.2 ± 0.1	-13.9 ± 0.1	-5.6 ± 0.1	-23.3 ± 0.1
T1 5.5 cm	-26.7 ± 0.1	-24.7 ± 0.1	-22.7 ± 0.1	-21.3 ± 0.1	-6.3 ± 0.1	-23.6 ± 0.1
T1 18.5 cm	-25.9 ± 0.1	-24.0 ± 0.1	-22.6 ± 0.1	-21.6 ± 0.1	-9.5 ± 0.1	-6.1 ± 0.1
T2 0.5 cm	-25.7 ± 0.1	-23.6 ± 0.1	-22.0 ± 0.1	-19.9 ± 0.1	-4.7 ± 0.1	-22.9 ± 0.1
T2 5.5 cm	-26.5 ± 0.1	-24.8 ± 0.1	-23.0 ± 0.1	-22.0 ± 0.1	-21.1 ± 0.1	-23.1 ± 0.1
T2 15.5 cm	-28.0 ± 0.1	-26.6 ± 0.1	-25.4 ± 0.1	-24.4 ± 0.1	-4.0 ± 0.1	-20.2 ± 0.1
T3 0.5 cm	-25.3 ± 0.1	-23.7 ± 0.1	-22.0 ± 0.1	-18.7 ± 0.1	-4.1 ± 0.1	-20.6 ± 0.1
T3 5.5 cm	-26.2 ± 0.1	-24.2 ± 0.1	-22.6 ± 0.1	-20.5 ± 0.1	-12.6 ± 0.1	-23.4 ± 0.1
T3 19.5 cm	-26.3 ± 0.1	-24.2 ± 0.1	-22.6 ± 0.1	-21.2 ± 0.1	-8.0 ± 0.1	-3.7 ± 0.1

206

207 3.3. Ramped oxidation and incubation comparison

208 Figure 1 presents a comparison of the ^{14}C content of the RO temperature fractions and respired
 209 CO_2 from the same soils during aerobic laboratory incubations (Houston et al. 2024b). These
 210 comparisons show that for each of the 0.5 cm depth samples, the ^{14}C content of the respired CO_2
 211 was greater than the ^{14}C content of any of the RO temperature fractions in the same soils (Fig. 1).
 212 For the 5.5 cm depth samples, the ^{14}C content of the CO_2 respired in the incubations was
 213 approximately equivalent to the ^{14}C content of the 150-325°C RO temperature fraction (Fig. 1).
 214 For T2 15.5 cm, the ^{14}C content of the respired CO_2 was also closest to the 150-325°C RO
 215 temperature fraction (Fig. 1). For the T1 18.5 cm and T3 19.5 cm samples, the ^{14}C contents of the
 216 incubation CO_2 were depleted relative to the 150-325°C RO temperature fraction for both
 217 samples, and instead, were closest to the 325-425°C and 425-500°C RO temperature fractions,
 218 respectively (Fig. 1).

219 3.4. Activation Energy

220 μE ranged from 157.50-170.97 kJ/mol for the 0.5 cm depth samples, 159.97-165.32 kJ/mol for the
 221 5.5 cm depth samples, and 154.38-160.44 kJ/mol for the deepest samples (T1 18.5 cm, T2 15.5
 222 cm, T3 19.5 cm. Table 3). σE ranged from 23.16-35.83 kJ/mol for the 0.5 cm depth samples, 22.16-
 223 25.25 kJ/mol for the 5.5 cm depth samples, and 21.43-23.51 kJ/mol for the deepest samples
 224 (Table 3). Between the three depth increments, there were no significant changes in μE or σE
 225 (Table 1. ANOVA; $p = 0.47$ and 0.37 , respectively).

226 *Table 3. μE and σE for each sample.*

	μE (kJ/mol)	σE (kJ/mol)
T1 0.5 cm	170.97	35.83
T1 5.5 cm	159.97	22.16
T1 18.5 cm	160.44	22.72
T2 0.5 cm	160.47	23.16
T2 5.5 cm	165.32	25.25
T2 15.5 cm	154.38	21.43
T3 0.5 cm	157.50	24.01
T3 5.5 cm	162.31	24.44
T3 19.5 cm	160.13	23.51

227

228 Table 4 shows μfE and the associated σfE for each thermal fraction. μfE ranged from 131.04-
229 133.23 kJ/mol for 150-325 °C, 156.83-157.78 kJ/mol for 325-425 °C, 176.14-177.79 kJ/mol for
230 425-500 °C, 185.44-199.19 kJ/mol for 500-650 °C, and 213.06-247.75 kJ/mol for 650-800 °C
231 (Table 4). σfE ranged from 7.33-8.71 kJ/mol for 150-325 °C, 9.83-10.23 kJ/mol for 325-425 °C,
232 6.88-8.83 kJ/mol for 425-500 °C, 3.68-16.04 kJ/mol for 500-650 °C, and 1.83-10.94 kJ/mol for 650-
233 800 °C (Table 4). μfE and σfE both varied significantly between the thermal fractions, increasing
234 sequentially (Kruskal-Wallis, $p = 0.001$ and 0.001 , respectively).

235

236 *Table 4. μfE and σfE for each RO temperature fraction for each sample.*

	μfE (σfE) (kJ/mol)				
	150-325°C	325-425°C	425-500°C	500-650°C	650-800°C
T1 0.5 cm	132.43 (7.33)	157.52 (10.17)	177.79 (7.32)	199.19 (16.04)	242.42 (10.94)
T1 5.5 cm	133.23 (8.07)	157.00 (10.13)	177.07 (7.58)	191.06 (7.87)	213.06 (2.12)
T1 18.5 cm	131.90 (8.62)	157.60 (9.83)	176.93 (7.83)	189.53 (6.70)	239.73 (6.73)
T2 0.5 cm	132.10 (8.21)	157.42 (10.08)	177.23 (7.38)	191.39 (10.62)	226.84 (6.81)
T2 5.5 cm	132.15 (8.71)	157.11 (10.01)	177.68 (8.83)	195.80 (7.95)	224.56 (4.55)
T2 15.5 cm	131.04 (8.46)	156.83 (10.23)	176.69 (6.88)	185.44 (3.68)	247.74 (1.83)
T3 0.5 cm	131.59 (7.48)	157.33 (10.07)	176.14 (7.07)	193.65 (12.46)	231.21 (10.04)
T3 5.5 cm	133.05 (8.28)	157.67 (10.14)	177.19 (7.70)	191.13 (9.11)	236.57 (4.29)
T3 19.5 cm	131.73 (8.38)	157.78 (10.00)	176.71 (7.34)	191.7 (10.53)	232.23 (9.69)

237

238 **4. Discussion**

239 Soils are complex mixtures of many different OC sources and ages, with different vulnerabilities
 240 to decomposition and turnover. In this study, we aimed to improve our understanding of the
 241 carbon cycling of saltmarsh soils by measuring the ^{13}C and ^{14}C content of thermally-fractionated
 242 soil carbon pools, and comparing these results to the ^{14}C content of biologically evolved CO_2 from
 243 the same soils (Houston et al., 2024b).

244 **4.1. Carbon provenance of ramped oxidation CO_2 fractions**

245 The first three RO temperature fractions (150-325°C, 325-425°C, 425-500°C) were derived solely
 246 from OC sources, as IC begins to breakdown from ca. 550°C (Hemingway et al., 2017b). CO_2 from
 247 the 500-650°C and 650-800°C fractions may, however, have been evolved from a mix of OC and
 248 IC sources. The IC contents of the studied soils (0.11-0.48%) were low relative to OC contents
 249 (4.18-7.71%), and IC makes only 1.95-10.48% of the total soil C pool for these samples (Table A2).

250 IC could have been removed from our saltmarsh soil samples to allow complete analysis of the
251 soil OC pool, and many R(P)O studies have taken this approach (Bao et al., 2019b; Hemingway et
252 al., 2017b; Luk et al., 2021; Stoner et al., 2023; Williams and Rosenheim, 2015). However, our
253 samples have low IC contents (Table A2), and acid-treatment, which is required to remove IC from
254 samples, can cause losses of labile OC (Bao et al., 2019a). Indeed, in Hemingway et al. (2017),
255 acid treatment of samples prior to RO resulted in a shift of 4 % Modern ^{14}C , which could change
256 one of our samples from having a pre-bomb ^{14}C content to a post-bomb ^{14}C content, or vice-
257 versa. A similar shift in ^{14}C content for our samples could seriously impact the interpretations in
258 our study, and our ability to compare the ^{14}C content of the CO_2 respired from bulk (untreated)
259 soils in the incubation experiments (Houston et al., 2024) to the ^{14}C content of the RO fractions.
260 The soils in the incubation experiments were also not decarbonated as the acid-treatment would
261 have affected soil respiration processes and made the results incomparable to in-situ soil
262 degradation processes (Houston et al., 2024b).

263 **4.2. ^{14}C content of ramped oxidation CO_2 fractions**

264 The ^{14}C -RO content decreased over the four thermal fractions (150-325 °C, 325-425 °C, 425-500
265 °C, 500-650 °C. Fig. 1), implying that ^{14}C -depleted OC had a greater thermal recalcitrance than
266 ^{14}C -enriched OC for these saltmarsh soil samples. Since the ^{14}C content of each RO fraction was
267 <100 % Modern (Table 1), each of the OC reactivity pools were likely to be predominantly
268 composed of carbon sequestered from the atmosphere before the 1963 ^{14}C bomb-spike caused
269 by atmospheric nuclear weapons testing, although we cannot completely discount some
270 contributions from post-bomb carbon (Hajdas et al., 2021). Nevertheless, using ^{14}C content as
271 an estimate of the age of the OC we can infer that the older (^{14}C -depleted) OC has a greater
272 thermal recalcitrance than young OC for these samples, which is consistent with previous
273 studies on the thermal reactivity of carbon stored in soils and sediments (e.g., Bao et al., 2019b;
274 Luk et al., 2021; Plante et al., 2013; Stoner et al., 2023).

275 The results suggest inhomogeneity within at least one of the temperature fractions for each
276 sample as, although there were no post-bomb ^{14}C contents for the incubation or RO samples
277 (Table 1), there is likely to be a fraction of post-bomb (post-AD1955) OC in at least one of the
278 temperature fractions. Autochthonous OC sequestration (post-bomb) at this accreting saltmarsh
279 (Hajdas et al., 2021; Smeaton et al., 2024) may become obscured by contributions from pre-
280 bomb (pre-AD1955) OC. Observing the decline in ^{14}C content with increasing temperature (Fig.
281 1), we hypothesise that, if present, this mixing of pre- and post-bomb C most likely occurred in
282 the 150-325°C fraction.

283 As the oldest (most ^{14}C -depleted) C had the greatest thermal recalcitrance (Fig. 1), this
284 emphasises that saltmarshes accumulating greater amounts of older (^{14}C -depleted) OC will
285 likely provide the most thermally recalcitrant OC stores, and saltmarshes accumulating greater
286 proportions of contemporary OC, either through in-situ production or young allochthonous
287 components, contain soil OC stores which are of greater thermal lability (Komada et al., 2022;
288 Van de Broek et al., 2018). However, the ^{14}C contents of the lowest temperature RO fraction (81-
289 98 % Modern; Table 1) highlight that although ^{14}C content decreases with decreasing thermal
290 reactivity (Fig. 1), thermally labile OC can still be aged (at least hundreds of years old) for these
291 soils. Due to the often anaerobic and non-eroding conditions of buried sediments, saltmarshes
292 can therefore be stores of old, but thermally labile carbon. Of course, the thermal recalcitrance
293 of OC is not necessarily related to biological turnover time, as this is also related to the prevailing
294 environmental conditions (Schmidt et al., 2011; Spivak et al., 2019).

295 **4.3. ^{13}C content of ramped oxidation CO_2 fractions**

296 ^{13}C -RO increased sequentially with the thermal fractions (Fig. 2), due to greater contributions
297 from relatively ^{13}C -enriched C sources from the higher temperature thermal fractions. The ^{13}C -RO
298 contents of the 150-650 °C fractions were each typical of OC sources (Leng and Lewis, 2017),
299 whereas the ^{13}C -RO contents of the 650-800 °C fraction were mostly typical of at least a partial
300 contribution from an IC source, with the exception of T2 5.5 cm and T3 5.5 cm (Table 2) (Brand et
301 al., 2014; Ramnarine et al., 2012). As IC can begin to evolve from 550 °C, it is possible that a mix
302 of OC and IC sources was present in the 500-650 °C thermal fractions.

303 As ^{13}C -RO increased with temperature (Fig. 2, Table 2), ^{13}C -enriched OC had a greater thermal
304 recalcitrance than ^{13}C -depleted OC for these samples. Previous work has demonstrated that >80
305 % of the OC accumulating at Skinflats saltmarsh is autochthonous/terrestrial in origin (Miller et
306 al., 2023), with limited contributions from marine OC. The thermally recalcitrant OC was
307 potentially composed of a greater amount of OC which has undergone microbial decomposition
308 as this process tends to enrich the degraded OC in ^{13}C (Boström et al., 2007; Etcheverría et al.,
309 2009; Luk et al., 2021; Sanderman and Grandy, 2020; Soldatova et al., 2024; Stoner et al., 2023).
310 The thermally recalcitrant OC may instead/also have been composed of more different OM
311 compounds (e.g., lignins, aromatics) than the more thermally labile OC (e.g., carbohydrates,
312 lipids) (Sanderman and Grandy, 2020). It is also possible that methodological artefacts, such as
313 kinetic fractionation, influenced the ^{13}C -RO contents. Kinetic fractionation is explained by
314 different carbon isotopes evolving as CO_2 from the soil sample at different rates during the
315 ramped heating (Hemingway et al., 2017a). Kinetic fractionation would cause the ^{13}C content of

316 the evolved CO₂ to increase linearly with temperature (Hemingway et al., 2017a), and we cannot
317 rule out this artefact. Hemingway et al. (2017a) determined that kinetic fractionation was not an
318 important factor in their RPO procedure, but we used a different set-up (described in Garnett et
319 al., 2023).

320 **4.4. Changes in the isotopic content of ramped oxidation CO₂ fractions with depth**

321 The isotopic composition of the evolved CO₂ did not vary significantly with depth for any of the
322 temperature fractions. The lack of an increase in the age (¹⁴C-depletion) of soil C with sample
323 depth is unusual, as typically C undergoes a burial process, and previous work has shown
324 diagenetic ageing of saltmarsh soils with depth as young OC is turned over faster than old OC
325 (Komada et al., 2022; Van de Broek et al., 2018).

326 Compared to other UK saltmarshes, Skinflats has relatively high C accumulation rates (Miller et
327 al., 2023; Smeaton et al., 2024). Depleted ¹⁴C contents of the OC accumulating at the Skinflats
328 saltmarsh (Houston et al., 2024b) imply that a proportion of the OC being buried may already
329 have been aged at the time of deposition on the marsh surface, as the marsh formed in the 1930's
330 (Miller et al., 2023). The combination of high carbon accumulation rates and depleted soil ¹⁴C
331 contents implies that the Skinflats saltmarsh accumulates a high proportion of old, most likely
332 allochthonous OC. Some of the aged, allochthonous OC may have undergone significant
333 microbial processing and degradation prior to its accumulation in the saltmarsh soil. As the OM
334 is degraded, and the energetically favourable components are consumed, the resulting OM
335 becomes increasingly thermally recalcitrant (Luk et al., 2021; Sanderman and Grandy, 2020;
336 Soldatova et al., 2024). The accumulation of a high proportion of degraded OC on the Skinflats
337 saltmarsh may therefore explain the lack of observed change in the isotopic composition of the
338 soil OC pools with depth. This interpretation is supported by the lack of change in both the
339 amount and the proportion of CO₂ evolved from each change temperature fraction with depth
340 (ANOVAs, $p > 0.05$. Table A3).

341 Not all old OC is degraded or thermally recalcitrant, and our results show that the Skinflats
342 saltmarsh is also a store of old (¹⁴C-depleted), thermally labile OC (Fig. 1). Old OC can be
343 thermally labile if it 'ages' (is stored) in an environment with low decomposition rates, e.g., a
344 peatland (Dean et al., 2023), prior to transport and accumulation into the saltmarsh. There are
345 extensive peatlands in the Skinflats catchment, many of which are degrading (Lilly et al., 2012).
346 Regardless of the age and degradation state of the OC deposited onto the marsh surface, as it
347 gets buried it will undergo a degree of microbial processing and degradation in the saltmarsh soil

348 (Luk et al., 2021), but that process is potentially less prevalent at Skinflats than saltmarshes
349 accumulating younger, less degraded OC.

350 Through isotopic analysis of saltmarsh soils partitioned using ramped oxidation, we have
351 determined that increased thermal recalcitrance is related to older (^{14}C -depleted; Fig. 1), more
352 degraded/microbially derived (^{13}C -enriched; Fig. 2) soil C. These findings are consistent with
353 previous research on the thermal reactivity of soil and sediment C, which have found that in most
354 cases, more energy is required (higher temperature/ μE) to decompose older (^{14}C -depleted),
355 degraded/microbially derived (^{13}C -enriched) C than younger (^{14}C -enriched), less processed (^{13}C -
356 depleted) C (e.g., Bao et al., 2019b; Plante et al., 2013; Stoner et al., 2023), including one
357 saltmarsh study (Luk et al., 2021).

358 **4.5. Comparison of biologically and thermally evolved CO_2**

359 As the biological turnover time of OC is related to the prevailing environmental conditions as well
360 as thermal reactivity, the isotopic composition of the most biologically- and thermally-reactive
361 saltmarsh soil OC pools may not be the same. To determine if this is the case, or not, we
362 compared the isotopic composition of the RO thermal reactivity fractions to the isotopic
363 composition of the CO_2 that was evolved biologically during incubations of equivalent samples
364 (Houston et al., 2024b) (Fig. 1).

365 Figure 1 shows that for each of the 0.5 cm depth samples, the ^{14}C content of the CO_2 respired in
366 the aerobic laboratory experiments was ^{14}C -enriched relative to any of the RO temperature
367 fractions, which was also the case for the T3 5.5 cm sample (Table 3). The relative ^{14}C -enrichment
368 of the biologically respired CO_2 compared to the thermally evolved CO_2 was likely caused by
369 inhomogeneity in the OC thermal reactivity pools, as each defined thermal reactivity pool may be
370 composed of multiple OC sources of variable age and composition. As thermal recalcitrance is
371 related to ^{14}C -depletion for these samples (Fig. 1), we hypothesise that for saltmarsh soil samples
372 producing respired CO_2 that was ^{14}C -enriched relative to any of the RO fractions (T1 0.5 cm, T2
373 0.5 cm, T3 0.5 cm, T3 5.5 cm; Table 1, Fig. 1), that this CO_2 was biologically-produced from an OC
374 pool within the most thermally labile RO fraction (150-325°C). Thus, we suggest that even within
375 the 150-325 °C RO fraction there are pools of even younger OC, but that they are masked by older,
376 ^{14}C -depleted OC. Similar findings of mixing within thermal fractions has been reported in previous
377 RPO work (e.g., Rosengard et al., 2025; Rosenheim et al., 2008).

378 The ^{14}C content of respired CO_2 from the 5.5 cm depth samples tended to be closer to the ^{14}C
379 content of the lowest temperature (150-325°C) RO fraction (Fig. 1), implying that for these
380 samples the biologically evolved CO_2 was from a thermally labile OC pool. The T2 15.5 cm

381 respired CO₂ sample was also similar in ¹⁴C content to the lowest temperature RO fraction,
382 whereas respired CO₂ from the slightly deeper T1 18.5 cm and T3 19.5 cm samples was ¹⁴C-
383 depleted relative to the 150-325°C RO fraction, instead aligning closer to the higher temperature
384 RO fractions (Fig. 1). The biologically evolved CO₂ from T1 18.5 cm and T3 19.5 cm were therefore
385 potentially derived from less thermally labile OC pools than the other samples, although it is
386 possible that the thermally labile pools were composed of multiple OC sources with different ¹⁴C
387 contents. The ¹⁴C content of the CO₂ evolved from the aerobic incubations of T1 18.5 cm and T3
388 19.5 cm was hypothesized to have been derived from an inorganic C source due to the enriched
389 ¹³C contents of -6.1‰ and -3.7‰, respectively (Houston et al., 2024b). As IC biological turnover
390 times are controlled by different factors than OC (Van Dam et al., 2021), and the remainder of the
391 samples were determined to evolve from OC substrates, this is likely to explain why the ¹⁴C
392 content of the CO₂ evolved from the aerobic incubation experiments for T1 18.5 cm and T3 19.5
393 cm did not align with the lowest temperature (most thermally labile) RO fraction (Fig. 1).
394 Therefore, there was a clear depth trend in the relationship between the ¹⁴C content of CO₂
395 respired in the aerobic incubation experiments and the ¹⁴C content of RO fractions of the same
396 bulk soils. Degradation of some of the thermally labile OM components during burial may reduce
397 the range of differently aged OC sources within the most thermally labile RO fraction for the
398 deeper samples in this study.

399 For seven out of nine samples (T1 18.5 cm and T3 19.5 cm being the outliers), the ¹⁴C content of
400 the CO₂ evolved from the aerobic laboratory incubations was closest to the ¹⁴C content of the
401 150-325°C RO temperature fraction. Therefore, even though the CO₂ evolved from the aerobic
402 incubation experiments was determined to be from a predominantly aged, allochthonous OC
403 source (Houston et al., 2024b), it can now also be shown to be derived from a predominantly
404 thermally labile OC pool (Fig. 1).

405 We did not attempt to relate the ¹³C-RO to the ¹³C content of the CO₂ respired in the incubation
406 experiments, due to the potential for microbial fractionation during the incubation experiments
407 which can change the ¹³C content of the respired CO₂ and the resulting soil OC (Soldatova et al.,
408 2024; Werth and Kuzyakov, 2010). In contrast, ¹⁴C results are normalised using the measured δ¹³C
409 values and are therefore immune to such isotopic fractionation effects.

410 **4.6. Implications**

411 Our results show that aged (presumed allochthonous), thermally labile OC stored in saltmarsh
412 soils remains vulnerable to loss to the atmosphere upon habitat drainage. Saltmarsh soils usually
413 exist in low-oxygen, tidally-inundated conditions which slow decomposition of OC (Chapman et

414 al., 2019), but many saltmarshes globally have been drained (and their soils subsequently
415 oxidised) to convert them for land uses such as housing developments and agriculture (Bromberg
416 and Bertness, 2005; Campbell et al., 2022; Morris et al., 2012). In the Forth Estuary, where the
417 Skinflats saltmarsh is located, as much as 50% of the intertidal area has been converted to
418 agricultural land since 1600, often involving the drainage of saltmarshes (Hansom and
419 McGlashan, 2008).

420 Protecting saltmarshes from degradation following drainage is listed as an eligible activity for
421 generating carbon credits for blue carbon ecosystem (BCE) projects (VERRA, 2023) and there is
422 significant potential for climate mitigation by avoided emissions from protecting vulnerable
423 stocks of soil OC in BCEs (Goldstein et al., 2020; Griscom et al., 2017; Kwan et al., 2025; Sasmito
424 et al., 2025). Similarly, the re-creation of saltmarsh habitat through managed realignment
425 (rewetting by tidal inundation) of historic saltmarsh habitats which were previously reclaimed for
426 land use purposes (e.g., agriculture) could reduce (and possible reverse) the emissions of aged
427 OC to the atmosphere, both locally to Skinflats, and globally.

428 The evidence for the respiration of thermally labile, allochthonous OC from saltmarsh soils in a
429 drainage degradation scenario demonstrates that at least this fraction of allochthonous OC could
430 be counted as additional in carbon crediting projects and National GHG Inventories. Because
431 allochthonous OC can account for up to 90 % of saltmarsh soil carbon (Komada et al., 2022), the
432 inclusion of allochthonous OC (or even a fraction of it) would significantly increase the climate
433 mitigation awarded to blue carbon projects (as carbon credits, or contributions to National GHG
434 Inventories) (Houston et al., 2024a).

435 As the bioavailable OC respired in the experiments of Houston et al. (2024b) was (in most cases)
436 from a predominantly thermally labile OC pool, and ^{14}C -RO decreased (C became older) with
437 increasing temperature (thermal recalcitrance), RO measurements could be useful for
438 characterising the turnover times of OC pools for saltmarsh soils exposed to oxic conditions
439 (drainage degradation scenario). The use of thermally defined OC pools to characterize OC
440 turnover times for saltmarsh soils would require a modelling advancement to constrain
441 degradation rates and residence times. Such efforts are not within the scope of this study but
442 could inform additionality/permanence in these saltmarsh systems. Experimentally defined
443 turnover times of OC thermal reactivity pools could, for example, provide a more robust approach
444 than inclusion/exclusion of allochthonous OC from saltmarsh 'blue carbon' projects (Houston et
445 al., 2024a).

446 Further research is needed to determine if the relationship between biological and thermal
447 lability exists for different degradation scenarios such as nutrient enrichment, as OC turnover
448 time is related to the environmental conditions as well as the thermal lability of the OC pools.
449 Similarly, these experiments would need to be replicated for a wider range of saltmarshes (high
450 and low latitude saltmarshes, different typologies), as there are likely to be differences in OC
451 turnover in different systems.

452 The samples used for this study were from the low marsh zone only, but it is likely that the thermal
453 reactivity of the Skinflats saltmarsh soil C will vary spatially across the marsh, as the proportion
454 of OC sources has been shown to be variable across saltmarshes (Middelburg et al., 1997). Given
455 our findings that old (^{14}C -depleted) OC has greater thermal recalcitrance than young (^{14}C -
456 enriched) OC (Fig. 1), we anticipate that higher marsh zones, which typically have greater
457 proportions of autochthonous OC than lower marsh zones (Spohn et al., 2013), would contain a
458 greater proportion of thermally labile OC. However, it is important to recognise that some of the
459 young (^{14}C -enriched), autochthonous OC in saltmarsh soils can also be thermally recalcitrant.
460 As well as marsh zonation, we expect that the proportion of OC sources (and associated mix of
461 thermal reactivities) would also vary with proximity to marsh creeks which redistribute
462 autochthonous and allochthonous C across the saltmarsh habitat (Middelburg et al., 1997; Reed
463 et al., 1999). In previously published work we showed that Skinflats accumulates OC of a much
464 greater 'age' (depleted soil ^{14}C contents) than two other saltmarshes in Scotland (Houston et al.,
465 2024b).

466 In this paper we have determined that age (^{14}C -content) is related to the thermal recalcitrance of
467 saltmarsh soil OC. We therefore speculate that sites accumulating younger OC would have more
468 thermally labile soil OC than sites accumulating older OC, like Skinflats, with wider implications
469 for the risks to these vulnerable stores of soil carbon from human disturbances.

470 **5. Conclusions**

471 This is the first study on saltmarsh soils to employ the ramped oxidation method. We show that
472 old (^{14}C -depleted) carbon dominates the thermally recalcitrant OC pools. The thermally labile OC
473 pools are also aged (^{14}C -depleted) compared to the contemporary atmosphere but are younger
474 than the thermally recalcitrant OC pools. These results highlight the role of saltmarshes as mixed
475 stores of both old, thermally recalcitrant OC, as well as younger, thermally labile OC.

476 We present the first comparison of the bioavailability (CO_2 evolved from incubation experiments;
477 Houston et al., 2024) and the thermal reactivity (RO) of saltmarsh soil OC. We show that aged,

478 allochthonous CO₂ evolved from saltmarsh soils exposed to oxic conditions (Houston et al.,
 479 2024b) are from a predominantly thermally labile OC pool. As saltmarsh soils exist mostly in low
 480 oxygen, waterlogged conditions, management interventions to limit their exposure to elevated
 481 oxygen availability may protect and conserve these stores of thermally labile OC and provide a
 482 climate abatement service. Therefore, we recommend that thermally labile allochthonous OC
 483 stored in saltmarsh soils should be counted as additional in some carbon crediting projects and
 484 National GHG Inventories.

485 Appendix A

486 *Table A1. Additional ¹⁴C measurement from the 650-800 °C. ¹⁴C was measured at the Scottish*
 487 *Universities Environmental Research Centre Accelerator Mass Spectrometer (AMS) Laboratory.*
 488 *δ¹³C (relative to Vienna PDB standard) was measured using isotope ratio mass spectrometry on*
 489 *a Delta V (Thermo, Germany) and used to normalize the ¹⁴C results to a δ¹³C = -25‰, which*
 490 *were reported as %Modern ¹⁴C (i.e., Fraction modern × 100). Errors are reported to one*
 491 *standard deviation from the mean.*

Sample ID	% Modern ¹⁴ C
Skin T1 0.5 cm 650-800 °C	79.75 ± 0.50

492

493

494 *Table A2. Soil carbon properties measured on equivalent sub-samples prior to the RO*
 495 *procedure, as reported in Houston et al. (2024). Total organic carbon (TOC), Total carbon (TC) for*
 496 *the soil samples were measured by a SoliTOC analyser (Elementar Analysensysteme, Hanau,*
 497 *Germany). ¹⁴C was measured at the Scottish Universities Environmental Research Centre*
 498 *Accelerator Mass Spectrometer (AMS) Laboratory. δ¹³C (relative to Vienna PDB standard) was*
 499 *measured using isotope ratio mass spectrometry on a Delta V (Thermo, Germany) and used to*
 500 *normalize the ¹⁴C results to a δ¹³C = -25‰, which were reported as %Modern ¹⁴C (i.e., Fraction*
 501 *modern × 100). Errors are reported to one standard deviation from the mean.*

Sample ID	TOC (%)	TIC (%)	TC (%)	% Modern ¹⁴ C	δ ¹³ C
SK T1 0.5 cm	4.1	0.48	4.58	47.49 ± 0.23	-23.5 ± 0.1
SK T1 5.5 cm	4.96	0.11	5.06	45.03 ± 0.20	-24.5 ± 0.1
SK T1 18.5 cm	4.8	0.39	5.18	41.36 ± 0.19	-23.8 ± 0.1
SK T2 0.5 cm	4.71	0.16	4.87	31.47 ± 0.15	-22.2 ± 0.1
SK T2 5.5 cm	4.23	0.13	4.36	43.69 ± 0.21	-24.1 ± 0.1
SK T2 15.5 cm	7.56	0.15	7.71	50.93 ± 0.24	-25.1 ± 0.1
SK T3 0.5 cm	5.37	0.12	5.49	47.03 ± 0.22	-23.7 ± 0.1
SK T3 5.5 cm	4.06	0.11	4.18	44.15 ± 0.21	24.0 ± 0.1
SK T3 19.5 cm	5.23	0.12	5.35	44.48 ± 0.21	-24.1 ± 0.1

502

503 *Table A3. Percentage (%) carbon evolved for each RO temperature fraction for each sample, and*
 504 *the relative contribution (%) to the total C evolved over the CO₂ collection temperature interval*
 505 *(150-650 °C)*

	% Carbon (% of Total Evolved CO ₂)				
	150-325 °C	325-425 °C	425-500 °C	500-650 °C	150-650 °C
T1 0.5 cm	1.42 (34.64)	1.17 (26.90)	1.07 (24.60)	0.69 (15.86)	4.35
T1 5.5 cm	1.44 (29.94)	1.59 (33.06)	1.11 (23.08)	0.67 (13.93)	4.81
T1 19.5 cm	1.48 (3.58)	1.43 (29.55)	1.31 (27.07)	0.62 (12.81)	4.84
T2 0.5 cm	1.45 (30.33)	1.30 (27.20)	1.44 (30.13)	0.59 (12.34)	4.78
T2 5.5 cm	1.09 (24.55)	1.13 (25.45)	1.12 (25.23)	1.1 (24.77)	4.44
T2 15.5 cm	2.66 (32.40)	2.60 (31.67)	2.12 (25.82)	0.83 (10.11)	8.21
T3 0.5 cm	1.98 (35.93)	1.6 (29.04)	1.38 (25.05)	0.55 (9.98)	5.51
T3 5.5 cm	1.13 (27.49)	1.32 (32.12)	1.08 (26.28)	0.58 (14.11)	4.11
T3 19.5 cm	1.48 (29.72)	1.75 (35.14)	1.11 (22.29)	0.64 (12.85)	4.98

506

507 **Data Availability**

508 All data presented in this manuscript is available in the main text and appendices.

509 **Author Contribution Statement**

510 A.H. undertook the study, fieldwork, sample processing, data acquisition, and wrote the first draft
 511 of the manuscript. M.G. conducted the laboratory procedures with the help of A.H. A.H., W.A.,
 512 and M.G. contributed to designing the study, fieldwork, and laboratory analyses. W.A., M.G., and
 513 J.S. oversaw the study and contributed to writing and revision of the manuscript.

514 **Competing Interests**

515 The authors declare that they have no conflict of interest.

516 **Acknowledgements**

517 We thank Jo Smith (University of Aberdeen) for her comments and edits on the first draft of this
 518 manuscript. We thank the NERC SUPER DTP for funding the PhD through which this research
 519 was undertaken (NE/S007342/1). We acknowledge support from the National Environmental
 520 Isotope Facility in funding the ¹⁴C measurements for this study under grant NE/S011587/1
 521 (allocation numbers 2594.1022, 2709.1023). WENA also acknowledges support provided by the
 522 HORIZON-CL5-2023-D1-02-02 grant C-BLUES, Innovation to advance the evidence base for
 523 reporting of Blue Carbon inventories and greenhouse gas fluxes in coastal wetlands. Thanks are
 524 extended to Chloe Bates for assisting with sample collection. Finally, we thank the editor and
 525 both reviewers for their comments which have improved this manuscript.

526 **Reference List**

- 527 Ascough, P., Bompard, N., Garnett, M. H., Gulliver, P., Murray, C., Newton, J.-A., and Taylor, C.:
528 ¹⁴C measurement of samples for environmental science applications at the National
529 Environmental Isotope Facility (NEIF) Radiocarbon Laboratory, SUERC, UK, *Radiocarbon*, 66,
530 1020–1031, <https://doi.org/10.1017/RDC.2024.9>, 2024.
- 531 Bao, R., McNichol, A. P., Hemingway, J. D., Gaylord, M. C. L., and Eglinton, T. I.: Influence of
532 Different Acid Treatments on the Radiocarbon Content Spectrum of Sedimentary Organic
533 Matter Determined by RPO/Accelerator Mass Spectrometry, *Radiocarbon*, 61, 395–413,
534 <https://doi.org/10.1017/RDC.2018.125>, 2019a.
- 535 Bao, R., Zhao, M., McNichol, A., Wu, Y., Guo, X., Haghypour, N., and Eglinton, T. I.: On the Origin
536 of Aged Sedimentary Organic Matter Along a River-Shelf-Deep Ocean Transect, *Journal of*
537 *Geophysical Research: Biogeosciences*, 124, 2582–2594,
538 <https://doi.org/10.1029/2019JG005107>, 2019b.
- 539 Bianchi, T. S., Mayer, L. M., Amaral, J. H. F., Arndt, S., Galy, V., Kemp, D. B., Kuehl, S. A., Murray,
540 N. J., and Regnier, P.: Anthropogenic impacts on mud and organic carbon cycling, *Nat. Geosci.*,
541 1–11, <https://doi.org/10.1038/s41561-024-01405-5>, 2024.
- 542 Boström, B., Comstedt, D., and Ekblad, A.: Isotope fractionation and ¹³C enrichment in soil
543 profiles during the decomposition of soil organic matter, *Oecologia*, 153, 89–98,
544 <https://doi.org/10.1007/s00442-007-0700-8>, 2007.
- 545 Brand, W. A., Coplen, T. B., Vogl, J., Rosner, M., and Prohaska, T.: Assessment of international
546 reference materials for isotope-ratio analysis (IUPAC Technical Report), *Pure and Applied*
547 *Chemistry*, 86, 425–467, <https://doi.org/10.1515/pac-2013-1023>, 2014.
- 548 Bromberg, K. D. and Bertness, M. D.: Reconstructing New England salt marsh losses using
549 historical maps, *Estuaries*, 28, 823–832, <https://doi.org/10.1007/BF02696012>, 2005.
- 550 Campbell, A. D., Fatoyinbo, L., Goldberg, L., and Lagomasino, D.: Global hotspots of salt marsh
551 change and carbon emissions, *Nature*, 1–6, <https://doi.org/10.1038/s41586-022-05355-z>, 2022.
- 552 Chapman, S. K., Hayes, M. A., Kelly, B., and Langley, J. A.: Exploring the oxygen sensitivity of
553 wetland soil carbon mineralization, *Biology Letters*, 15, 20180407,
554 <https://doi.org/10.1098/rsbl.2018.0407>, 2019.
- 555 Dean, J. F., Billett, M. F., Turner, T. E., Garnett, M. H., Andersen, R., McKenzie, R. M., Dinsmore, K.
556 J., Baird, A. J., Chapman, P. J., and Holden, J.: Peatland pools are tightly coupled to the
557 contemporary carbon cycle, *Global Change Biology*, n/a, e16999,
558 <https://doi.org/10.1111/gcb.16999>, 2023.
- 559 Etcheverría, P., Huygens, D., Godoy, R., Borie, F., and Boeckx, P.: Arbuscular mycorrhizal fungi
560 contribute to ¹³C and ¹⁵N enrichment of soil organic matter in forest soils, *Soil Biology and*
561 *Biochemistry*, 41, 858–861, <https://doi.org/10.1016/j.soilbio.2009.01.018>, 2009.
- 562 Garnett, M. H., Pereira, R., Taylor, C., Murray, C., and Ascough, P. L.: A New Ramped Oxidation-
563 ¹⁴C Analysis Facility at the NEIF Radiocarbon Laboratory, East Kilbride, UK, *Radiocarbon*, 65,
564 1213–1229, <https://doi.org/10.1017/RDC.2023.96>, 2023.

565 Gerald, N. R., Ortega, A., Serrano, O., Macreadie, P. I., Lovelock, C. E., Krause-Jensen, D.,
566 Kennedy, H., Lavery, P. S., Pace, M. L., Kaal, J., and Duarte, C. M.: Fingerprinting Blue Carbon:
567 Rationale and Tools to Determine the Source of Organic Carbon in Marine Depositional
568 Environments, *Frontiers in Marine Science*, 6, 263, <https://doi.org/10.3389/fmars.2019.00263>,
569 2019.

570 Goldstein, A., Turner, W. R., Spawn, S. A., Anderson-Teixeira, K. J., Cook-Patton, S., Fargione, J.,
571 Gibbs, H. K., Griscom, B., Hewson, J. H., Howard, J. F., Ledezma, J. C., Page, S., Koh, L. P.,
572 Rockström, J., Sanderman, J., and Hole, D. G.: Protecting irrecoverable carbon in Earth's
573 ecosystems, *Nat. Clim. Chang.*, 10, 287–295, <https://doi.org/10.1038/s41558-020-0738-8>,
574 2020.

575 Granse, D., Wanner, A., Stock, M., Jensen, K., and Mueller, P.: Plant-sediment interactions
576 decouple inorganic from organic carbon stock development in salt marsh soils, *Limnology and*
577 *Oceanography Letters*, n/a, <https://doi.org/10.1002/lol2.10382>, 2024.

578 Griscom, B. W., Adams, J., Ellis, P. W., Houghton, R. A., Lomax, G., Miteva, D. A., Schlesinger, W.
579 H., Shoch, D., Siikamäki, J. V., Smith, P., Woodbury, P., Zganjar, C., Blackman, A., Campari, J.,
580 Conant, R. T., Delgado, C., Elias, P., Gopalakrishna, T., Hamsik, M. R., Herrero, M., Kiesecker, J.,
581 Landis, E., Laestadius, L., Leavitt, S. M., Minnemeyer, S., Polasky, S., Potapov, P., Putz, F. E.,
582 Sanderman, J., Silvius, M., Wollenberg, E., and Fargione, J.: Natural climate solutions,
583 *Proceedings of the National Academy of Sciences*, 114, 11645–11650,
584 <https://doi.org/10.1073/pnas.1710465114>, 2017.

585 Hajdas, I., Ascough, P., Garnett, M. H., Fallon, S. J., Pearson, C. L., Quarta, G., Spalding, K. L.,
586 Yamaguchi, H., and Yoneda, M.: Radiocarbon dating, *Nat Rev Methods Primers*, 1, 1–26,
587 <https://doi.org/10.1038/s43586-021-00058-7>, 2021.

588 Hemingway, J. D.: rampedpyrox: Open-source tools for thermoanalytical data analysis, 2016-,
589 2016.

590 Hemingway, J. D., Galy, V. V., Gagnon, A. R., Grant, K. E., Rosengard, S. Z., Soulet, G., Zigah, P. K.,
591 and McNichol, A. P.: Assessing the Blank Carbon Contribution, Isotope Mass Balance, and
592 Kinetic Isotope Fractionation of the Ramped Pyrolysis/Oxidation Instrument at NOSAMS,
593 *Radiocarbon*, 59, 179–193, <https://doi.org/10.1017/RDC.2017.3>, 2017a.

594 Hemingway, J. D., Rothman, D. H., Rosengard, S. Z., and Galy, V. V.: Technical note: An inverse
595 method to relate organic carbon reactivity to isotope composition from serial oxidation,
596 *Biogeosciences*, 14, 5099–5114, <https://doi.org/10.5194/bg-14-5099-2017>, 2017b.

597 Hemingway, J. D., Rothman, D. H., Grant, K. E., Rosengard, S. Z., Eglinton, T. I., Derry, L. A., and
598 Galy, V. V.: Mineral protection regulates long-term global preservation of natural organic carbon,
599 *Nature*, 570, 228–231, <https://doi.org/10.1038/s41586-019-1280-6>, 2019.

600 Houston, A., Kennedy, H., and Austin, W. E. N.: Additionality in Blue Carbon Ecosystems:
601 Recommendations for a Universally Applicable Accounting Methodology, *Global Change*
602 *Biology*, 30, e17559, <https://doi.org/10.1111/gcb.17559>, 2024a.

603 Houston, A., Garnett, M. H., and Austin, W. E. N.: Blue carbon additionality: New insights from
604 the radiocarbon content of saltmarsh soils and their respired CO₂, *Limnology and*
605 *Oceanography*, n/a, <https://doi.org/10.1002/lno.12508>, 2024b.

- 606 Howard, J., Sutton-Grier, A. E., Smart, L. S., Lopes, C. C., Hamilton, J., Kleypas, J., Simpson, S.,
607 McGowan, J., Pessarrodona, A., Alleway, H. K., and Landis, E.: Blue carbon pathways for climate
608 mitigation: Known, emerging and unlikely, *Marine Policy*, 156, 105788,
609 <https://doi.org/10.1016/j.marpol.2023.105788>, 2023.
- 610 Komada, T., Bravo, A., Brinkmann, M.-T., Lu, K., Wong, L., and Shields, G.: “Slow” and “fast” in
611 blue carbon: Differential turnover of allochthonous and autochthonous organic matter in
612 minerogenic salt marsh sediments, *Limnology and Oceanography*, n/a,
613 <https://doi.org/10.1002/lno.12090>, 2022.
- 614 Kwan, V., Friess, D. A., Sarira, T. V., and Zeng, Y.: Permanence risks limit blue carbon financing
615 strategies to safeguard Southeast Asian mangroves, *Commun Earth Environ*, 6, 1–8,
616 <https://doi.org/10.1038/s43247-025-02035-4>, 2025.
- 617 Leng, M. J. and Lewis, J. P.: C/N ratios and Carbon Isotope Composition of Organic Matter in
618 Estuarine Environments, in: *Applications of Paleoenvironmental Techniques in Estuarine
619 Studies*, edited by: Weckström, K., Saunders, K. M., Gell, P. A., and Skilbeck, C. G., Springer
620 Netherlands, Dordrecht, 213–237, https://doi.org/10.1007/978-94-024-0990-1_9, 2017.
- 621 Lilly, A., Baggaley, N., and Donnelly, D.: Map of soil organic carbon in top soils of Scotland, 2012.
- 622 Luk, S. Y., Todd-Brown, K., Eagle, M., McNichol, A. P., Sanderman, J., Gosselin, K., and Spivak, A.
623 C.: Soil Organic Carbon Development and Turnover in Natural and Disturbed Salt Marsh
624 Environments, *Geophysical Research Letters*, 48, e2020GL090287,
625 <https://doi.org/10.1029/2020GL090287>, 2021.
- 626 Macreadie, P. I., Anton, A., Raven, J. A., Beaumont, N., Connolly, R. M., Friess, D. A., Kelleway, J.
627 J., Kennedy, H., Kuwae, T., Lavery, P. S., Lovelock, C. E., Smale, D. A., Apostolaki, E. T., Atwood, T.
628 B., Baldock, J., Bianchi, T. S., Chmura, G. L., Eyre, B. D., Fourqurean, J. W., Hall-Spencer, J. M.,
629 Huxham, M., Hendriks, I. E., Krause-Jensen, D., Laffoley, D., Luisetti, T., Marbà, N., Masque, P.,
630 McGlathery, K. J., Magonigal, J. P., Murdiyarso, D., Russell, B. D., Santos, R., Serrano, O.,
631 Silliman, B. R., Watanabe, K., and Duarte, C. M.: The future of Blue Carbon science, *Nature
632 Communications*, 10, 3998, <https://doi.org/10.1038/s41467-019-11693-w>, 2019.
- 633 Macreadie, P. I., Costa, M. D. P., Atwood, T. B., Friess, D. A., Kelleway, J. J., Kennedy, H.,
634 Lovelock, C. E., Serrano, O., and Duarte, C. M.: Blue carbon as a natural climate solution, *Nat
635 Rev Earth Environ*, 2, 826–839, <https://doi.org/10.1038/s43017-021-00224-1>, 2021.
- 636 Middelburg, J. J., Nieuwenhuize, J., Lubberts, R. K., and van de Plassche, O.: Organic Carbon
637 Isotope Systematics of Coastal Marshes, *Estuarine, Coastal and Shelf Science*, 45, 681–687,
638 <https://doi.org/10.1006/ecss.1997.0247>, 1997.
- 639 Miller, L. C., Smeaton, C., Yang, H., and Austin, W. E. N.: Carbon accumulation and storage
640 across contrasting saltmarshes of Scotland, *Estuarine, Coastal and Shelf Science*, 108223,
641 <https://doi.org/10.1016/j.ecss.2023.108223>, 2023.
- 642 Morris, J. T., Edwards, J., Crooks, S., and Reyes, E.: Assessment of carbon sequestration
643 potential in coastal wetlands, in: *Recarbonization of the Biosphere: Ecosystems and the Global
644 Carbon Cycle*, 517–532, https://doi.org/10.1007/978-94-007-4159-1_24, 2012.
- 645 Noyce, G. L., Smith, A. J., Kirwan, M. L., Rich, R. L., and Magonigal, J. P.: Oxygen priming induced
646 by elevated CO₂ reduces carbon accumulation and methane emissions in coastal wetlands,
647 *Nat. Geosci.*, 16, 63–68, <https://doi.org/10.1038/s41561-022-01070-6>, 2023.

- 648 Peltre, C., Fernández, J. M., Craine, J. M., and Plante, A. F.: Relationships between Biological and
649 Thermal Indices of Soil Organic Matter Stability Differ with Soil Organic Carbon Level, *Soil*
650 *Science Society of America Journal*, 77, 2020–2028, <https://doi.org/10.2136/sssaj2013.02.0081>,
651 2013.
- 652 Plante, A. F., Fernández, J. M., Haddix, M. L., Steinweg, J. M., and Conant, R. T.: Biological,
653 chemical and thermal indices of soil organic matter stability in four grassland soils, *Soil Biology*
654 *and Biochemistry*, 43, 1051–1058, <https://doi.org/10.1016/j.soilbio.2011.01.024>, 2011.
- 655 Plante, A. F., Beaupré, S. R., Roberts, M. L., and Baisden, T.: Distribution of Radiocarbon Ages in
656 Soil Organic Matter by Thermal Fractionation, *Radiocarbon*, 55, 1077–1083,
657 <https://doi.org/10.1017/S0033822200058215>, 2013.
- 658 R Core Team: R: A language and environment for statistical computing., 2022.
- 659 Ramnarine, R., Wagner-Riddle, C., Dunfield, K. E., and Voroney, R. P.: Contributions of
660 carbonates to soil CO₂ emissions, *Can. J. Soil. Sci.*, 92, 599–607,
661 <https://doi.org/10.4141/cjss2011-025>, 2012.
- 662 Reed, D. J., Spencer, T., Murray, A. L., French, J. R., and Leonard, L.: Marsh surface sediment
663 deposition and the role of tidal creeks: Implications for created and managed coastal marshes,
664 *J Coast Conserv*, 5, 81–90, <https://doi.org/10.1007/BF02802742>, 1999.
- 665 Rosengard, S. Z., Mauro S. Moura, J., Spencer, R. G. M., Johnson, C., McNichol, A., Boehman, B.,
666 and Galy, V.: The Thermal Reactivity and Molecular Diversity of Particulate Organic Carbon in the
667 Amazon River Mainstem, *Journal of Geophysical Research: Biogeosciences*, 130,
668 e2024JG008660, <https://doi.org/10.1029/2024JG008660>, 2025.
- 669 Rosenheim, B. E., Day, M. B., Domack, E., Schrum, H., Benthien, A., and Hayes, J. M.: Antarctic
670 sediment chronology by programmed-temperature pyrolysis: Methodology and data treatment,
671 *Geochemistry, Geophysics, Geosystems*, 9, <https://doi.org/10.1029/2007GC001816>, 2008.
- 672 Saintilan, N., Rogers, K., Mazumder, D., and Woodroffe, C.: Allochthonous and autochthonous
673 contributions to carbon accumulation and carbon store in southeastern Australian coastal
674 wetlands, *Estuarine, Coastal and Shelf Science*, 128, 84–92,
675 <https://doi.org/10.1016/j.ecss.2013.05.010>, 2013.
- 676 Sanderman, J. and Grandy, A. S.: Ramped thermal analysis for isolating biologically meaningful
677 soil organic matter fractions with distinct residence times, *SOIL*, 6, 131–144,
678 <https://doi.org/10.5194/soil-6-131-2020>, 2020.
- 679 Sasmito, S. D., Taillardat, P., Adinugroho, W. C., Krisnawati, H., Novita, N., Fatoyinbo, L., Friess,
680 D. A., Page, S. E., Lovelock, C. E., Murdiyarso, D., Taylor, D., and Lupascu, M.: Half of land use
681 carbon emissions in Southeast Asia can be mitigated through peat swamp forest and mangrove
682 conservation and restoration, *Nat Commun*, 16, 740, [https://doi.org/10.1038/s41467-025-](https://doi.org/10.1038/s41467-025-55892-0)
683 [55892-0](https://doi.org/10.1038/s41467-025-55892-0), 2025.
- 684 Schmidt, M. W. I., Torn, M. S., Abiven, S., Dittmar, T., Guggenberger, G., Janssens, I. A., Kleber,
685 M., Kögel-Knabner, I., Lehmann, J., Manning, D. A. C., Nannipieri, P., Rasse, D. P., Weiner, S., and
686 Trumbore, S. E.: Persistence of soil organic matter as an ecosystem property, *Nature*, 478, 49–
687 56, <https://doi.org/10.1038/nature10386>, 2011.

688 Smeaton, C., Garrett, E., Koot, M. B., Ladd, C. J. T., Miller, L. C., McMahon, L., Foster, B., Barlow,
689 N. L. M., Blake, W., Gehrels, W. R., Skov, M. W., and Austin, W. E. N.: Organic carbon
690 accumulation in British saltmarshes, *Science of The Total Environment*, 926, 172104,
691 <https://doi.org/10.1016/j.scitotenv.2024.172104>, 2024.

692 Soldatova, E., Krasilnikov, S., and Kuzyakov, Y.: Soil organic matter turnover: Global implications
693 from $\delta^{13}\text{C}$ and $\delta^{15}\text{N}$ signatures, *Science of The Total Environment*, 912, 169423,
694 <https://doi.org/10.1016/j.scitotenv.2023.169423>, 2024.

695 Spivak, A. C., Sanderman, J., Bowen, J. L., Canuel, E. A., and Hopkinson, C. S.: Global-change
696 controls on soil-carbon accumulation and loss in coastal vegetated ecosystems, *Nat. Geosci.*,
697 12, 685–692, <https://doi.org/10.1038/s41561-019-0435-2>, 2019.

698 Spohn, M., Babka, B., and Giani, L.: Changes in soil organic matter quality during sea-influenced
699 marsh soil development at the North Sea coast, *CATENA*, 107, 110–117,
700 <https://doi.org/10.1016/j.catena.2013.02.006>, 2013.

701 Stoner, S. W., Schrumppf, M., Hoyt, A., Sierra, C. A., Doetterl, S., Galy, V., and Trumbore, S.: How
702 well does ramped thermal oxidation quantify the age distribution of soil carbon? Assessing
703 thermal stability of physically and chemically fractionated soil organic matter, *Biogeosciences*,
704 20, 3151–3163, <https://doi.org/10.5194/bg-20-3151-2023>, 2023.

705 Van Dam, B. R., Zeller, M. A., Lopes, C., Smyth, A. R., Böttcher, M. E., Osburn, C. L., Zimmerman,
706 T., Pröfrock, D., Fourqurean, J. W., and Thomas, H.: Calcification-driven CO₂ emissions exceed
707 “Blue Carbon” sequestration in a carbonate seagrass meadow, *Science Advances*, 7, eabj1372,
708 <https://doi.org/10.1126/sciadv.abj1372>, 2021.

709 Van de Broek, M., Vandendriessche, C., Poppelmonde, D., Merckx, R., Temmerman, S., and
710 Govers, G.: Long-term organic carbon sequestration in tidal marsh sediments is dominated by
711 old-aged allochthonous inputs in a macrotidal estuary, *Global Change Biology*, 24, 2498–2512,
712 <https://doi.org/10.1111/gcb.14089>, 2018.

713 VERRA: VM0033 Methodology for Tidal Wetland and Seagrass Restoration, v2.1, 2023.

714 Werth, M. and Kuzyakov, Y.: ^{13}C fractionation at the root–microorganisms–soil interface: A
715 review and outlook for partitioning studies, *Soil Biology and Biochemistry*, 42, 1372–1384,
716 <https://doi.org/10.1016/j.soilbio.2010.04.009>, 2010.

717 Williams, E. K. and Rosenheim, B. E.: What happens to soil organic carbon as coastal marsh
718 ecosystems change in response to increasing salinity? An exploration using ramped pyrolysis,
719 *Geochemistry, Geophysics, Geosystems*, 16, 2322–2335,
720 <https://doi.org/10.1002/2015GC005839>, 2015.

721

722

723

724

725

726

727

728

729

730

731

732

733

734

735

736

737